ANALYSIS OF THE GRINDING FORCE COMPONENTS AND SURFACE ROUGHNESS IN GRINDING WITH THE USE OF A GLASS-CRYSTALLINE BONDED GRINDING WHEEL

Analiza składowych siły szlifowania oraz chropowatości powierzchni podczas szlifowania z użyciem ściernicy ze spoiwem szklanokrystalicznym

Marcin ŻÓŁKOŚ ORCID: 0000-0003-0377-1428

DOI: 10.15199/160.2020.1.7

Abstract: The article concerns an investigation of 100Cr6 steel surface peripheral grinding process with glass-crystalline bonded grinding wheels. More precisely the investigation of surface roughness parameters and grinding force components in relation to different dressing overlap ratio, feed rate and grinding depths values. Seven different values of dressing overlap ratio have been used to determine influence of dressing overlap ratio to grinding force and surface roughness. After determining the stable range of dressing overlap ratio, other tests were conducted with eleven different values of feed rate and two values of grinding depth to determine how they shape the grinding force components and surface roughness parameters. The machining has been performed using a CNC surface grinding machine, together with a surface grinding wheel and up grinding strategy. Additional NI equipment was used for grinding force data acquisition. The surface roughness was assessed using two parameters (*Ra, Rz*). The contact measurements of surface roughness were carried out using the MarSurf PS 10 profilometer. The dresser effective width was measured with the use of AM7515MZT Dino-Lite microscope to ensure consistent values of dressing overlap ratio throughout the entire experiment. Significant impact of the dressing overlap ratios, feed rate and grinding depths on the grinding force components F_n and F_t*as* well as the roughness parameters *Ra* and *Rz* were obtained.
Keywords: grinding, grinding force components, surface roughness, dressing overlap ratio, glass-crystalline bond

Streszczenie: Artykuł dotyczy badań procesu szlifowania obwodowego stali 100Cr6 za pomocą ściernic o spoiwie szklanokrystalicznym. Dokładniej dotyczy badań parametrów chropowatości powierzchni i składowych siły szlifowania w odniesieniu do różnych wartości wskaźnika pokrycia przy obciąganiu, posuwu i głębokości szlifowania. Siedem różnych wartości wskaźnika pokrycia przy obciąganiu zostało wykorzystanych do określenia wpływu wskaźnika pokrycia na siłę szlifowania i chropowatość powierzchni. Po określeniu stabilnego zakresu wskaźnika pokrycia przy obciąganiu przeprowadzono kolejne badania z jedenastoma różnymi wartościami posuwu i dwiema wartościami głębokości szlifowania, aby określić ich wpływ na składowe siły szlifowania i parametry chropowatości powierzchni. Obróbka została wykonana przy użyciu szlifierki CNC do płaszczyzn wraz ze ścierniczą obwodową i strategią szlifowania przeciwbieżnego. Dodatkowo do pomiarów siły szlifowania zostało wykorzystane oprzyrządowanie NI. Chropowatość powierzchni została oceniona za pomocą dwóch parametrów (*Ra, Rz*). Pomiary stykowe chropowatości powierzchni przeprowadzono przy użyciu profilometru MarSurf PS 10. Czynna szerokość obciągacza była mierzona przy użyciu mikroskopu Dino-Lite AM7515MZT, aby zapewnić stałe wartości wskaźnika pokrycia przy obciąganiu w trakcie wszystkich wykonywanych badań. W efekcie uzyskano istotny wpływ wskaźnika pokrycia przy obciąganiu, posuwu i głębokości szlifowania na składowe siły szlifowania F_n i F_t oraz na parametry chropowatości *Ra* i *Rz*.
Słowa kluczowe: szlifowanie, składowe siły szlifowania, chropowatość powierzchni, wskaźnik pokrycia przy obciąganiu, spoiwo szklanokrystaliczne

Introduction

Grinding is a process of subtractive machining, which may have the character of a precise finishing machining or highly efficient subtractive machining [22, 23]. There are many types of grinding, such as, among others, surface peripheral and face grinding, longitudinal shafts grinding, hole grinding [23, 26]. In order to carry out the grinding process, it is necessary to use appropriate machine tools and grinding wheels.

Grinding is still one of the basic processes for finishing operations, where peripheral grinding is widely used for precise surface grinding. Grinding wheel wear, geometric accuracy and surface quality of workpiece are greatly influenced by grinding forces [25]. The ability to predict grinding force components is important in many aspects of grinding process optimization, monitoring and control [4]. In this context, research into the modeling and calculation of grinding forces is current, necessary and constantly being developed.

The main directions of the development of grinding processes can be divided into three main groups, such as hybrid processes, new kinematic varieties and modifications of grinding wheel structure. The development of abrasive tools is a complex issue including, among others, works on new abrasive materials and binders,

which together define the structure of grinding wheels. The possibility of influencing on the structure of a grinding wheel is also a modification of the existing types of binders or abrasive materials [15, 17, 18].

The basic task of the binder is to bond the abrasive grains in the abrasive tool. It determines the properties of the tool, proper maintenance of the abrasive grains, proper porosity, maintaining the shape accuracy of the grinding wheel and determines the dressing method [13, 26]. The bond therefore has a decisive influence on the grinding wheel active surface (GWAS), which is shaped both in the dressing process and in the grinding wheel self-sharpening process. One of the most widely used types of binders in tools with conventional abrasives are ceramic bonds [13, 15]. One of the variations of these binders is glass-crystalline binders, which are characterized by a different mechanism of propagation of cracks in the bridges of the binder in relation to glass binders. That characteristic translates into the ability of the binder to micro-chipping in a similar manner as it takes place in grains of microcrystalline sintered corundum [7, 9, 19].

Herman [5] and Herman et al. [6, 8] conducts research on the construction, production and physical proper-ties of glass-crystalline binders and the manufacturing of new varieties of glass-crystalline binders. Nadolny et al. [16, 19 – 21] conducts technological research on grinding wheels with glass-crystalline bond and grains of microcrystalline sintered alumina in the process of holes grinding. Other research on the production of different varieties of glass-crystalline binders [2, 10, 11, 14, 24] do not include extended and accurate technological research of abrasive tools with such binders in the process of peripheral surface grinding. This state of affairs determines the necessity of conducting research on glass-crystalline binders in the process of peripheral grinding of surfaces and their improvement.

Conducted experimental tests concerned the 100Cr6 surface peripheral grinding process with the use of innovative grinding wheels with glass-crystalline bond. Their goal was to determine the influence of dressing overlap ratio, feed rate, grinding depth on grinding force components and surface roughness parameters. So it would be possible to specify the dressing overlap value. Also to select feed rate and grinding depth values ranges for further more extended experiments.

Research methodology and experimental conditions

To accomplish that goal samples in the form of cuboids (length of 50 mm and width of 30 mm), made of 100Cr6 steel, were prepared and used as the workpieces in the conducted experiments. The samples were through hardened and tempered to 60 ±2 HRC hardness. The workpieces were machined on the test stand described in the subsection „The grinding process" and shown in Figure 1.

As the machining tool the Andre Abrasive Articles grinding wheel (type 7), was used, with a two-sided cylindrical recess A. The tested grinding wheel with designation M3X60H8VTHE-35 had medium sized abrasive grains (average grain size - 275 μm) made of monocrystalline corundum, with a 30% share of microcrystalline electro-corundum. The tool that was used for research was bonded with modified vitrified binder that has glass-crystalline structure.

The abovementioned material samples were machined and measured using the machining and measurement parameters, which are presented in Table 1. As the results of conducted experiments the grinding force components (normal *Fn* and tangential *Ft*) and surface roughness parameters (*Ra* and *Rz*) were acquired. Based on that results correlations between grinding force components/surface roughness parameters and dressing overlap ratio/feed rate/grinding depth were obtained.

• The grinding process

The experimental part of the research (mechanical machining) was carried out using the CNC test stand. The test stand (see Figure 1) was developed for the needs of the research revolved around grinding wheels with modified vitrified binders [3, 27]. The Geibel & Hotz GmbH FS 640 Z surface grinding machine was the main part of this test stand. The stand has been equipped with Kistler type 9121 piezoelectric dynamometer, Kistler Type 5019 A amplifier, NI CompactDAQ system and LabVIEW SignalExpress software that together allowed the measurement of grinding force components.

The stand was also equipped with a high pressure cooling system, in which a coolant in the form of a 5% synthetic emulsion was fed into the grinding zone, over the entire width of the grinding wheel, by means of a needle nozzle at a pressure of 1 MPa, which corresponded to a volumetric flow rate of 22 l/min [1, 12]. For coolant pressure readout and control there was pressure sensor installed and DC power supply with desktop multimeter added to the test stand.

The tests were carried out in the surface peripheral up grinding setup with constant grinding speed value and varying values of feed rate, grinding depth and dressing overlap ratio (refer to Table 1). Before each measure-ment pass, the dressing of the grinding wheel with single grain diamond dresser was performed with specific set of parameters, which are presented in Table 1. After dressing one machining pass was made with grinding depth 0.002 mm and feed rate 20000 mm/min to remove loose grains remaining after the sharpening process of

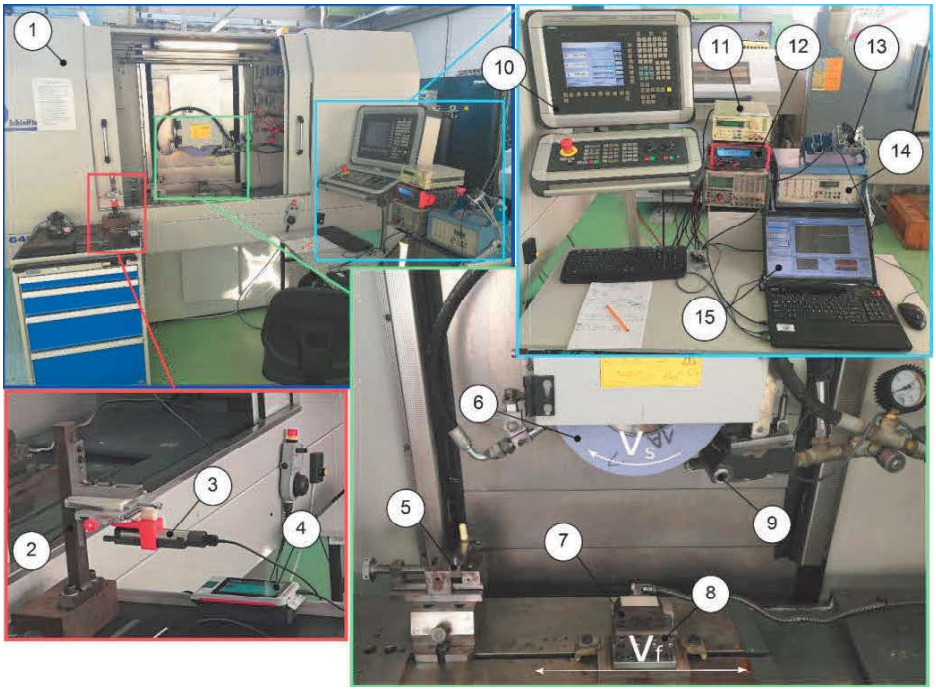

Fig. 1. Configuration of the test stand: 1 – G+H FS 640 Z surface grinding machine, 2 – mounting holder for profilometer drive unit,3 - MarSurf PS 10 profilometer drive unit, 4 - main unit of MarSurf PS 10 profilometer, 5 – diamond dresser, 6 – grinding wheel, 7 – workpiece, 8 – dynamometer, 9 – needle nozzle for coolant distribution, 10 – machine control panel, 11 – DC power supply, 12 – desktop multimeter for coolant pressure readout, 13 – NI CompactDAQ system, 14 – Kistler 5019 A amplifier, 15 – computer with LabVIEW SignalExpress software

the grinding wheel. Afterwards a machining pass took place, for which values of the normal and tangential component of the grinding force were recorded. After the measurement pass, ten sparking passes were made to provide a constant machining allowance for the next pass. Grinding was performed with specific technological parameters whose values are shown in the Table 1. Values of the grinding force components were recorded for each machining pass, which were repeated three times for one set of technological parameters.

- **Measurements of surface roughness parameters**

The measurements of surface roughness parameters were performed with the use of the MarSurf PS 10 profilometer directly at the surface grinding machine without removing workpieces from dynamometer (refer to Figure 1). Measurements were performed for all 18 different combinations of technological parameters values. Parameters of every roughness measurement are listed in Table 1. Three measurements replications of the analyzed surface roughness parameters *Ra* and *Rz* were carried out. They were done after every repetition of the machining pass with different set of technological parameters values. The surface roughness measurements were executed in perpendicular direction to the feed rate. A total number of 162 single surface roughness measurements were made for all the investigated technological parameters values combinations.

Table 1. Parameters of machining and measurement processes

Parameters of grinding process	Parameters of dressing process	Parameters of surface roughness measurement
Andre Abrasives Articles surface grinding wheel- 7-300x50x76.2 P150;F10;G10 M3X60H8VTHE-35 5% synthetic coolant mixed with water cutting fluid pressure, p = 1 MPa cutting fluid volumetric flow, q = 22 l/min grinding speed, v_c = 40 m/s feedrate, v_f = 4000 / 7000÷35000 mm/min grinding depth, a_e = 0.02 / 0.03 m	single-grain diamond dresser dressing peripheral speed, v_d = 25 m/s dressing depth, a_{ed} = 0.02 mm dressing overlap ratio, u_d = 1.5÷10 /4 dressing passes - 5	traversing length, l_t = 4.8 mm evaluation length, l_n = 4.0 mm max. probe tip radius, r_{tip} = 2 µm sampling length, lr = 0.8 mm scanning speed, v_t = 1.0 mm/s measurement resolution - 8 nm number of repetition - 3

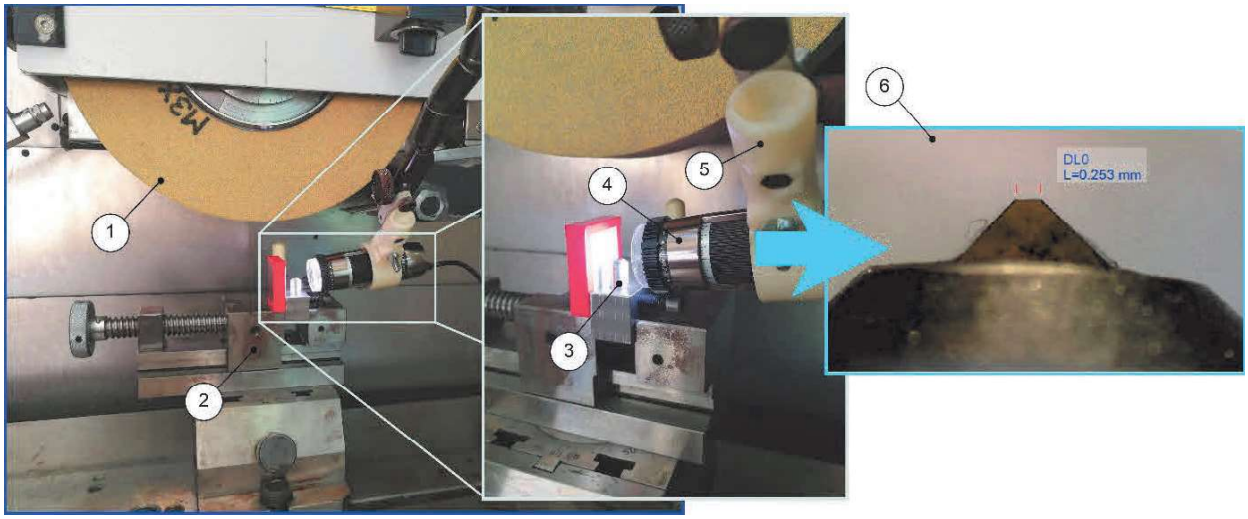

Fig. 2. Test stand configuration for diamond dresser measurements: 1 – grinding wheel, 2 – grinding vise, 3 – diamond dresser, 4 – AM7515MZT Dino-Lite portable microscope, 5 – adjustable holder, 6 – microscope diamond dresser view with width measurement result

- **Measurements of dresser effective contact width**

In order to achieve the specified U_d values, the width of the dresser was measured before each dressing process to adjust the feed rate of the grinding wheel at dressing to maintain the specified U_d value. Also, in some tests, where the U_d parameter remained constant, it was necessary to continuously check the width of the dresser. This was required to keep the value of this ratio constant. Therefore, the AM7515MZT Dino-Lite portable microscope was used to measure the width of the dresser before each dressing pass. The microscope was calibrated to read the correct width values before the measurements were taken. The microscope, when properly placed in the holder attached to the grinding wheel housing, allowed the evaluation of the condition of the dresser and measurements of the active dresser width in the grinding machine working area (see Figure 2). This eliminated the need to remove the dresser from the machine and to repeat after each measurement the setup steps on the machine.

The results and discussion

On figure 3 there are presented average values of the normal F_n and tangential F_t grinding force components in relation to dressing overlap ratio U_d.

Calculated confidence intervals for 3 measurement repetitions (per each of the grinding force component) executed at each different dressing overlap ratio value are shown on the graph. The applied significance level was 0.05. The obtained values of the F_n and F_t components indicate significant differences in grinding force components among different values of dressing overlap ratio. The lowest values were obtained for the smallest U_d value, which were 68 N for normal component and 31 N for tangential component. The highest values were obtained for the largest value of U_d ratio: 197 N and 83 N respectively. This corresponds to 190% increase for F_n component and 168% increase for F_t component. In both cases for normal and tangential components the positive correlation to dressing overlap ratio can be seen on the graph below. In addition, the local minimum of the force component values for a dressing overlap ratio of 3 can be observed.

For the smallest U_d ratio the lowest forces occur, because we get the most aggressive GWAS due to higher pulling forces in the dressing process. They are caused by the higher dressing feed rate (the lower the U_d ratio, the higher the dressing feed rate v_d). This results in a smaller contact area between the grains and the workpiece surface during cutting. While the dressing overlap ratio increases the dresser smoothes the grain surface by blunting rather than pulling it out or chipping. This translates into increased forces due to the increased contact area between the grains and the machined surface. For U_d ratio, we can indicate a stable

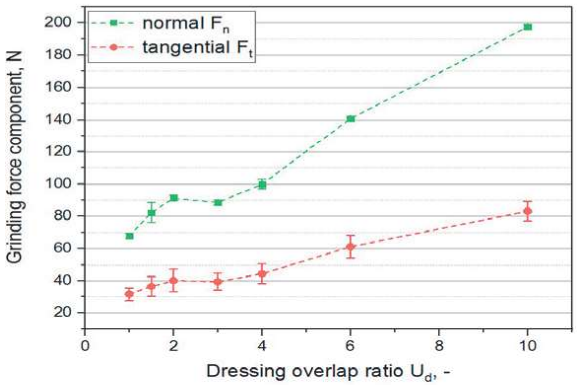

Fig. 3. The results of F_n/ F_t grinding force component measurements vs. dressing overlap ratio

range of values from 2 to 4. Smaller values should be ignored, as it will be difficult to maintain its exact value in this range (inaccuracy in measuring the width of the dresser), which can translate into cutting a helix line into a GWAS that will affect the quality of the grinded surface. In addition, in the range below 2 there is definitely the fastest wear of the dresser. On the other hand, values above 4 contribute to higher forces in the process, which can cause surface damage. Larger values of U_d ratio also increase significantly the time of the dressing process, which results in a longer total machining time.

Figure 4 indicates average values of the grinding force components in relation to feed rate v_f.

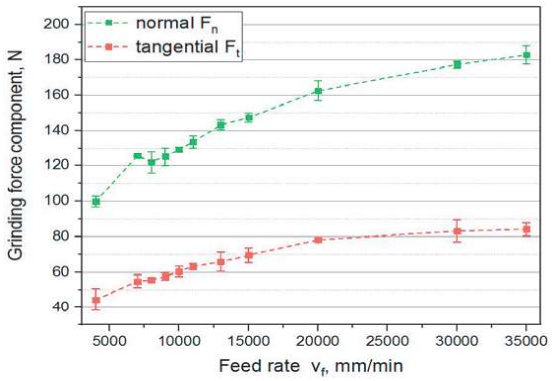

Fig. 4. The results of Fn / Ft grinding force component measurements vs. feed rate

This may be caused by the higher strength of the glass-crystalline bond compared to the traditional ceramic bond. The glass-crystalline bond requires higher forces to tear out and chip out the blunted grain. Therefore, in the range of v_f up to 20000 mm/min, dulled grains are kept in the binder all the time, causing an increase in forces. On the other hand, above v_f 20000 mm/min there are enough large forces that allow to occur the grinding wheel selfsharpening process and reduction of the forces value gradient for higher feed rates.

Figure 5 presents average values of the normal F_n and tangential F_t grinding force components in relation to grinding depth a_e.

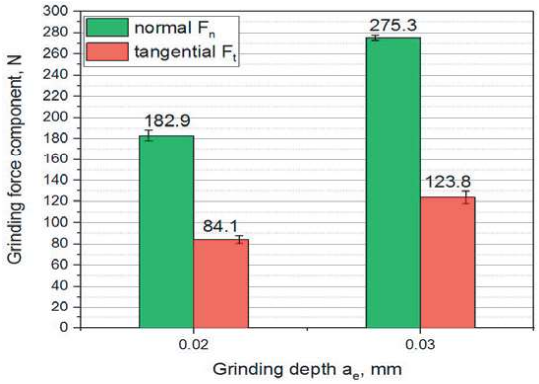

Fig. 5. The results of Fn and Ft grinding force component measurements vs. grinding depth

In the case of measurements of the impact of feed rate on the components of grinding forces, the conditions were adopted as for previous tests. The obtained values of the F_n and F_t components indicate significant differences in grinding force components among different values of feed rate. The lowest values were obtained for the feed rate of 4000 mm/min and the highest for the 35000 mm/min feed rate. The lowest values of F_n component and F_t component were 100 N and 44 N. The highest values were 183 N and 84 N accordingly. That corresponded to 83% increase for normal component and 91% for tangential component. As in figure 3, the above graph shows a small break of the normal grinding force component for a feed rate of 8000 mm/min. For both grinding force components the positive correlation to feed rate can be observed on the Figure 4.

The obtained graph of dependence of the grinding force component values confirms their dependence on the feed rate in grinding processes - increase of the forces values together with the feed rate increase. What is interesting, however, above the feed rate value of 20000 mm/min there does not occur a significant increase in grinding forces, which takes place in the range from 4000 to 20000 mm/min. This indicates that grinding wheels with this bond perform better in tougher conditions.

On the graph are also marked the calculated confidence intervals for 3 measurement repetitions (per each of the grinding force component) executed at two grinding depth values. The applied significance level was the same as in previous tests. The obtained values of the F_n and F_t components indicate significant differences in grinding force components among different values of grinding depth. The lower values were obtained for the ae equal to 0.02 mm, which were 183 N for normal component and 84 N for tangential component. The higher values were obtained for the 0.03 mm value of ae: 275 N and 124 N respectively. This corresponds to 50% increase for F_n component and 48% increase for F_t component. In both cases for normal and tangential components their values are bigger while grinding depth increases.

The graph above thus confirms the same dependence of forces from the grinding depth for grinding wheels with glass-crystalline bond and ceramic bond. However, in order to fully confirm this statement, additional research will be required in a wider range of grinding depth values.

Figure 6 presents average values of the *Ra* and *Rz* parameters in relation to overlap dressing ratio U_d.

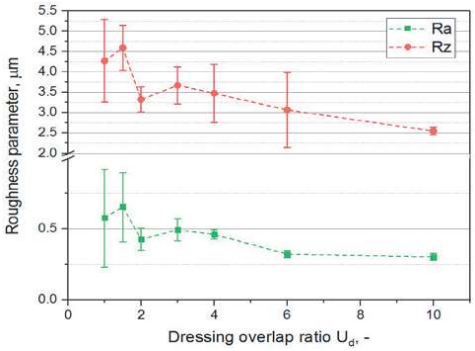

Fig. 6. The results of *Ra* / *Rz* parameter measurements vs. dressing overlap ratio

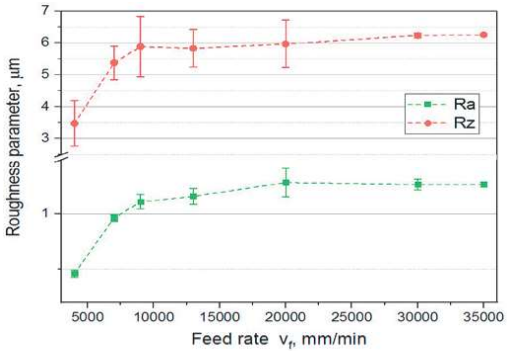

Fig. 7. The results of *Ra* / *Rz* parameter measurements vs. feed rate

The calculated confidence intervals for 7 different dressing overlap values (3 machining passes per each Ud value and 3 measurement repetitions per each machining pass) are shown on the graph. The applied significance level was 0.05. The obtained values of the *Ra* and *Rz* parameters indicate significant differences in surface roughness among different dressing overlap ratio values. The lowest roughness parameters values were obtained for the biggest U_d values, and the highest ones for the lowest U_d values.

On the above chart it can be observed that for smaller values of the dressing overlap ratio there are larger confidence intervals. It is especially visible for the obtained values of the roughness parameter *Ra*. For the results of the parameter *Rz*, the spread of results values is greater for the vast majority of measurement points. Due to the characteristics of this roughness parameter, the *Rz* parameter is more sensitive to single defects in the measured profile that interfere with the final result. This is confirmed by the previously determined stable U_d ratio range for the dressing overlap ratio dependence on the grinding force components. Of course, the surface roughness for higher values of the dressing overlap ratio is lower, but this results in a significant increase in the grinding force value. The obtained roughness dependence on the dressing overlap ratio allows us to determine the best value for further research. For value 4 we obtain the smallest spread of values for a given stable range of dressing overlap ratio. This may indicate a more stable process of dresser wear and reduced wear value for this exact value U_d.

Figure 7 presents average values of the *Ra* and *Rz* parameters in relation to feed rate v_f.

On the graph are also marked the calculated confidence intervals in the same way as in previous tests. The obtained values of the *Ra* and *Rz* parameters indicate significant differences in surface roughness among different feed rate values. The lowest roughness parameters values were obtained for the lowest v_f values, and the highest ones for the biggest v_f values.

In the graph above it can be observed that for *Ra* and *Rz* parameters from 9000 mm/min, the gradient of change of *Ra* and Rz values depending on the change of the feed rate is significantly reduced. This leads to very similar results for surface roughness parameters above the feed rate thresholds values given above. It may be associated with the phenomenon of micro-chipping of abrasive grains and glass-crystalline binder, which ensures stabilization of the GWAS profile, translating into stabilization of the roughness parameters *Ra* and *Rz*. Similarly as in the graph 6 for the results of the parameter *Rz* confidence intervals are larger for the vast majority of measurement points, compared to the results of the *Ra* parameter.

Figure 8 presents average values of the *Ra* and *Rz* parameters in relation to grinding depth a_e.

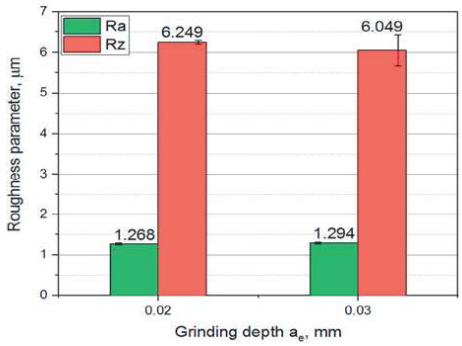

Fig. 8. The results of *Ra* / *Rz* parameter measurements vs. grinding depth

The calculated confidence intervals (the same significance level as stated before) for 3 measurements executed for each machining pass repetition at two grinding depth values are marked on the graph. The obtained values of the *Ra* and *Rz* parameters indicate no significant differences in surface roughness among different grinding depth values. The *Ra* roughness parameter values were practically the same for both grinding depth values. It was similar in the case of *Rz* parameter, but for grinding depth equal to 0.03 mm there was bigger confidence interval.

From the above obtained dependence of roughness parameters on grinding depth for grinding wheels with glass-crystalline bond it can be concluded that the grinding depth does not influence the roughness value. However, in order to confirm this thesis, it is necessary to perform more thorough research for a larger number of measuring points.

Conclusions

As the results of the study, the impact of the dressing overlap ratios, feed rate and grinding depths on the grinding force components F_n and F_t, as well as the roughness parameters *Ra* and *Rz* were obtained. The obtained results allow stating the following conclusions:

- For investigated grinding process the stable range for dressing overlap ratio is U_d = 2.0÷4.0.
- For further research, the ratio U_d = 4.0 have been selected due to the more stable process of dresser wear and smaller wear value during the grinding wheel sharpening process, which manifests itself in a smaller spread of *Ra* and *Rz* surface roughness parameter values as well as comparable grinding force components values compared to U_d values 2 or 3.
- Increase of dressing overlap ratio U_d from the lowest to the highest considered value results in 190% increase of normal force F_n and a 168% increase of tangential force F_t. In addition dressing overlap ratio increase results in increasing the surface roughness parameters *Ra* and *Rz*.
- Increase of feed rate from the lowest to the highest value results in 83% increase of normal force F_n and a 91% increase of tangential force F_t. For *Ra* and *Rz* parameters the increase of feed rate results in an initial increase in their value, but later on the stabilization of the surface parameters values occur.
- Increase of grinding depth by 0.01 mm results in 50% increase of normal grinding force component F_n and a 48% increase of tangential component F_t. Grinding depth increase does not significantly affect the change of surface roughness parameters.
- The selected overlap dressing value, for all the analyzed feed rates and grinding depths values, allowed *Ra* parameter values below 1.4 *μm*, *Rz* below 6.8 *μm* and normal grinding force components F_n values below 278 N, tangential component F_t below 130 N, to be obtained.

References

[1] Babiarz R., Żyłka Ł., Płodzień M. 2014. "Concept design of the high-pressure cooling system for the grinding of air alloys". Mechanik (87): 4–7.

[2] Chainikova A.S., Orlova L.A., Popovich N.V., Grashchenkov D.V., Lebedeva Y.E., Solntsev S.S. 2015. "Sr-anorthite glass ceramic with enhanced crack resistance, reinforced with silicon nitride particles". Russ. J. Appl. Chem. (88): 18–26.

[3] Habrat W., Żółkoś M., Świder J., Socha E. 2018. "Forces modeling in a surface peripheral grinding process with the use of various design of experiment (DoE)". Mechanik (91): 929–931.

[4] Hecker R.L., Liang S.Y., Wu X.J., Xia P., Jin D.G.W. 2007. "Grinding force and power modeling based on chip thickness analysis". Int J Adv Manuf Technol (33): 449–459.

[5] Herman D. 2006. "New generation of CBN grinding wheels bonded with glass-ceramic". Advances in Science and Technology (45): 1515–1519.

[6] Herman D., Okupski T., Walkowiak W. 2011. "Wear resistance glass-ceramics with a gahnite phase obtained in CaO-MgO-ZnO-Al2O3-B2O3-SiO2 system". Journal of the European Ceramic Society (31): 485–492.

[7] Herman D., Plichta J., Karpiński T. 1997. "Effect of glass-crystalline and amorphous binder application to abrasive tools made of microcrystalline alumina grains type SG". Wear (209): 213–218.

[8] Herman D., Pobol T., Walkowiak W. 2015. "Wpływ właściwości termicznych i mechanicznych spoiw szklanokrysta-licznych na mechanizm zużycia ściernic z pcBN". Mechanik (88): 126–131.

[9] Höland W., Beall G.H. 2012. "Glass-ceramic technology". John Wiley & Sons, Inc.

[10] Iordanova R.S., Milanova M.K., Aleksandrov L.I., Khanna A., Georgiev N. 2016. "Optical characterization of glass and glass- crystalline materials in the B2O3-Bi2O3-La2O3 system doped with Eu3+ ions". Bulg. Chem. Commun. (48): 11–16.

[11] Karamanov A., Kamusheva A., Karashanova D., Ranguelov B., Avdeev G. 2018. "Structure of glass--ceramic from Fe-Ni wastes". Materials Letters (223): 86–89.

[12] Kieraś S., Nadolny K., Wójcik R. 2015. "State in the art of cooling and lubrication of the machining zone in grind-ing processes". Mechanik (88): 204–211.

[13] Marinescu I.D., Rowe W.B., Dimitrov B., Ohmori H. 2013.Abrasives and abrasive tools. In Tribology of Abrasive Machining Processes (Second Edition), 243–311.William Andrew Publishing.

[14] Moreno M.B.P., Murillo-Gómez F., De Goes M. 2018. "Effect of different ceramic-primers and silanization--protocols on glass-ceramic bond strength". Dental Materials (34): e80–e81.

[15] Nadolny K. 2014. "State of the art in production, properties and applications of the microcrystalline sintered corun-dum abrasive grains". Int J Adv Manuf Technol (74): 1445–1457.

[16] Nadolny K. 2016. "Shaping the cutting ability of grinding wheels with zone-diversified structure". Proceedings of the Institution of Mechanical Engineers, Part B: Journal of Engineering Manufacture (230): 254–266.

[17] Nadolny K., Habrat W. 2017. "Potential for improving efficiency of the internal cylindrical grinding process by mod-ification of the grinding wheel structure—Part I: Grinding wheels made of conventional abrasive grains:". Proceed-ings of the Institution of Mechanical Engineers, Part E: Journal of Process Mechanical Engineering (231): 621–632.

[18] Nadolny K., Habrat W. 2017. "Potential for improving efficiency of the internal cylindrical grinding process by mod-ification of the grinding wheel structure—Part II: Grinding wheels made of superabrasive grains:". Proceedings of the Institution of Mechanical Engineers, Part E: Journal of Process Mechanical Engineering (231): 813–823.
[19] Nadolny K., Herman D. 2015. "Effect of vitrified bond microstructure and volume fraction in the grinding wheel on traverse internal cylindrical grinding of Inconel® alloy 600". The International Journal of Advanced Manufacturing Technology (81): 905–915.
[20] Nadolny K., Kapłonek W. 2015. "Identification of the tribological processes on the grinding wheel surface during the internal cylindrical grinding of 100Cr6 steel, based on SEM-EDS analysis". International Journal of Surface Sci-ence and Engineering (9): 298–313.
[21] Nadolny K., Kapłonek W., Ungureanu N. 2017. "Effect of macro-geometry of the grinding wheel active surface on traverse internal cylindrical grinding process". Journal of Mechanical and Energy Engineering (1): 15–22.
[22] Oczoś K.E., Habrat W. 2010. "Doskonalenie procesów obróbki ściernej. Cz. I. Quo vadis szlifowanie?". Mechanik (83): 449–452.
[23] Oczoś K.E., Habrat W. 2010. "Doskonalenie procesów obróbki ściernej. Cz. II. Wysokoefektywne ściernice i procesy szlifowania.". Mechanik (83): 517–529.
[24] Shi J., He F., Xie J., Liu X., Yang H. 2019. "Effect of heat treatments on the Li2O-Al2O3-SiO2-B2O3-BaO glass-ceramic bond and the glass-ceramic bond cBN grinding tools". International Journal of Refractory Metals and Hard Materials (78): 201–209.
[25] Tang J., Du J., Chen Y. 2009. "Modeling and experimental study of grinding forces in surface grinding". Journal of Materials Processing Technology (209): 2847–2854.
[26] Toenshoff H.K., Denkena B. 2013. "Basics of Cutting and Abrasive Processes". Springer.
[27] Żółkoś M., Habrat W., Świder J., Socha E. 2018. "Analysis of influence of the mono-crystalline corundum grinding wheel wear on grinding forces and roughness parameters in peripheral surface grinding of 100Cr6 steel". Mechanik (91): 702–704.

Mgr inż. Marcin Żółkoś

Rzeszow University of Technology, The Faculty of Mechanical Engineering and Aeronautics, al. Powstańców Warszawy 8, 35-959 Rzeszów, Poland
e-mail: markos@prz.edu.pl